A R C H I V E O F M E C H A N I C A L E N G I N E E R I N G

Volume 66 2019 Number 4

DOI: 10.24425/ame.2019.131355

Key words: flexoelectricity, surface effects, imperfections, resonance frequency, nanobeam

M. Bastanfar[1], S.A.H. Hosseini[2], R. Sourki[3], F. Khosravi[4]

Flexoelectric and surface effects on a cracked piezoelectric nanobeam: Analytical resonant frequency response

A nanoscale beam model containing defect under the piezoelectricity considering the surface effects and flexoelectricity is established on the framework of Euler-Bernoulli theory. The governing equations of motion and related boundary conditions are derived by using Hamilton's principle. The imperfect nanobeam is modeled by dividing the beam into two separate parts that are connected by a rotational and a longitude spring at the defect location. Analytical results on the free vibration response of the imperfect piezoelectric nanobeam exhibit that the flexoelectricity and the surface effects are sensitive to the boundary conditions, defect position, and geometry of the nanobeam. Numerical results are provided to predict the mechanical behavior of a weakened piezoelectric nanobeam considering the flexoelectric and surface effects. It is also revealed that the voltage, defect severity, and piezoelectric material have a critical role on the resonance frequency. The work is envisaged to underline the influence of surface effects and flexoelectricity on the free vibration of a cracked piezoelectric nanobeam for diverse boundary conditions. It should be mentioned, despite our R. Sourkiprevious works, an important class of piezoelectric materials used nowadays and called piezoelectric ceramics is considered in the current study.

1. Introduction

In the past decades, nanostructures have been extensively utilized in nano-electro-mechanical systems (NEMS) such as nano-resonators and nano-oscillators [1]. Combination of the piezoelectric and semiconducting properties of

✉ S.A.H. Hosseini, e-mail: hosseini@bzte.ac.ir

[1]Department of Mechanical Engineering, University of Zanjan, Zanjan, Iran.

[2]Department of Industrial, Mechanical and Aerospace Engineering, Buein Zahra Technical University, Buein Zahra, Qazvin, Iran.

[3]School of Engineering, The University of British Columbia, Kelowna, BC, V1V 1V7 Canada.

[4]Department of Aerospace Engineering, K.N. Toosi University of Technology, Tehran, Iran.

GaN, nano-rods, and ZnO nanostructures are essential for obtaining electricity from mechanical energy, and harvesting solar energy [2, 3]. ZnO nanowires have become a central factor in powering nano-devices by converting mechanical energy into electricity [4]. A fundamental application of some nanostructures such as piezoelectric field effect transistor (PE-FET) and nano-sensors made of ZnO nanowire are sensors for measuring forces [5]. They can also be used as a gate voltage for controlling the current flow [6]. However, there is evidence that nanostructures are size-dependent and have considerable impact on the static/dynamic response of the nanostructure. Chaipanich [7] revealed the size-dependent behavior of PZT-cement composites and demonstrated that the dielectric property of the composites enhances by PZT particle size. A size-dependent viscoelastic model was also extended for nanotube resonators by Farokhi and his colleagues [8]. The size-dependent behavior a clamped piezoelectric nano-plate was depicted by Zhang et al. under transverse vibration and bending [9]. Liang et al. [10], illustrated that the electromechanical coupling coefficient of the piezoelectric nanobeam under bending is size-dependent. The size-dependent vibration and bending analysis of a clamped piezoelectric circular nano-plate were presented using a modified Kirchhoff plate model by Yan [11]. Also, the variation of the resonant frequency was represented with the plate thickness and plate radius to thickness ratio was represented utilizing a modified Kirchhoff plate model.

Flexoelectricity, on the other hand, refers to an electrical polarization caused by a strain gradient (or inhomogeneous strain) that describes many electromechanical behaviors. It is a size-dependent effect, which becomes more prominent in nanostructures [12]. This property enables scientists to harvest energy from materials and makes it feasible to design self-powered sensors in nanoscale. According to the flexoelectricity theory and the strain gradient theory, a size-dependent bending model of an electro-elastic bi-layer nanobeam was considered under the open and closed circuit conditions. Recent work by several studies illustrate the size-dependency of the flexoelectricity and the strain gradient elastic effect [13]. An analytical solution for the deflection and rotation of the Timoshenko dielectric nanobeam model was obtained with the direct effect of flexoelectricity under various boundary conditions [14]. Results revealed that the flexoelectricity in the size-dependent electromechanical coupling response plays a vital role when the beam thickness is small. Yan and Jiang [15] determined the flexoelectric effect on the electro-elastic fields in the bending piezoelectric nanobeams with various boundary conditions while electrical and mechanical loads were applied to nanobeams. Simulation results depicted the fact that the flexoelectric effect on the elastic behavior of nanobeams depends on the boundary conditions and the electrical load. Furthermore, it was mentioned that the flexoelectricity has significant influence upon the contact stiffness and electric polarization of nanobeams while thickness is in nanoscale values.

Interestingly, when flexoelectricity is under consideration, surface effects commonly present a remarkable influence in predicting the size-dependency of piezo-

electric nanostructures [16]. Liang et al. [17], investigated the buckling and vibration of the piezoelectric nanowires considering the flexoelectricity and surface effects based on Euler-Bernoulli beam theory. It was found that the surface effects and flexoelectricity have a significant influence on Young's modulus, bending rigidity, critical buckling voltage, and the first resonance frequency of PZT and $BaTiO_3$ nanowires. A year later, using Timoshenko beam model with piezoelectric couple stress theory and flexoelectricity theory, a size-dependent static deformation and free vibration of the hinged-hinged piezoelectric nanobeam were presented by Tadi Beni [18]. Sourki et al. [19] analyzed free transverse vibration of a cracked microbeam, modeled by a rotational spring, on the basis of modified couple stress theory. They considered the impacts of crack position, Poisson's ratio, material length scale parameter as well as crack severity on natural frequencies. It has been investigated that the crack severity has a negative effect on natural frequency. Based on nonlocal modified couple stress theory incorporating surface effects, the nonlocal parameter, surface effect parameters and crack position were found to have prominent influences on stiffness and dynamic behavior of the weakened nanobeam [20].

Other than nanoscale beams, nanoscale shells and plates were the focus of many researchers [21–28]. Two-dimensional general equations of piezoelectric shells with nano-thickness were suggested by Zhang et al. [29] considering the surface effects. It was concluded that due to surface effects, the resonant frequencies of the piezoelectric cylindrical shell at nanoscale under an axisymmetric deformation and different boundary conditions are size dependent. A modified Kirchhoff plate model was extended by considering the residual surface stress, surface elasticity, surface piezoelectricity, and flexoelectricity to study the electro elastic responses and the free vibration of a piezoelectric nanoplate. The surface effects and flexoelectricity on the electromechanical coupling behaviors of the piezoelectric nano-plate is related to the plate dimensions and the electrical loading [30]. Yan and Jiang [31] discussed the surface effects on the size-dependent electro-elastic responses of the static bending and buckling behaviors of the piezoelectric nanoplate within Kirchhoff plate theory with different in-plane constraints. By considering the surface piezoelectricity, a piezoelectric ring under a prescribed potential has been studied by Huang and Yu [32]. Numerical results demonstrated an important effect of surface piezoelectricity on the electric and stress fields in the nanometer scale. The sinusoidal plate model was used to analyze the bending problem of a simply supported piezoelectric nanoplate considering the surface effect. Then, the influence of surface effects and electric loading on the displacement, electric potential, stress and electric displacement was reported under the uniform electromechanical loading [33]. In order to estimate the bending behavior of nanowires, a framework of high-order surface stresses based on the continuum theory of Euler– Bernoulli beams was served by Chiu and Chen [34]. The results indicated that, under a certain critical diameter size, high-order surface stresses have a highlighted influence on the bending behavior of nanowires.

There have been some studies on the defected nanostructures mostly on nanobeams showing the importance of the defect features on the response of nanostructures [19, 20, 35, 36]. A case in point is the work of Xiao et al. [37] on piezoelectric materials with an elliptical cavity based on surface effect subjected to the electromechanical load. The results revealed the size dependency of stress and electric displacement fields and the electro-elastic intensity factors with the nanometer cavity size. By considering surface effects, Wang and Wang [38] developed a nonlinear fracture mechanics analysis model for nanoscale piezoelectric double cantilever beam specimens. Simulation results indicated that the influence of the surface residual stress and negative surface elasticity upon the energy release rate depends on the length to thickness ratio of the piezoelectric double cantilever beam. The effect of crack face residual surface stress on the nanoscale fracture of an infinite piezoelectric medium considered by Nan and Wang [39]. The results showed that the electromechanical coupling fracture behavior of the piezoelectric materials is significantly affected by the residual surface effect.

As cited above, piezoelectric materials on nanoscale have widely used in diverse devices including sensors, actuators, energy harvesters due to their high electromechanical coupling, mechanical and physical properties. The literature reveals that the properties of piezoelectric nanomaterials depend on the particular-size and do not follow their bulk counterparts. The flexoelectricity also as a size-dependent property becomes more significant at the nanoscale that could strikingly affect the electromechanical coupling behavior of piezoelectric materials. It is clear that the capabilities of structures are reduced because of the existence of cracks or other defects. Thereby, the issue of cracking in the structures is interested in nano-scale dimensions. With regard to the fact that all modes of vibration do not equally contribute to the response of a structure, normally only those modes which have higher participation factors are considered. This assumption actually helps in simplifying the problem. In mechanical systems when the frequency of oscillations matches the natural frequency of vibration, mechanical resonance occurs and tend to absorb more energy than it does at other frequencies. It can lead to violent motions and disastrous failures in inappropriately constructed structures. Hence, the importance of considering it in order to avoiding resonance catastrophes is a major concern in every structure. Overall, there is little published study of nanoscale structures and previous studies have not dealt with the flexoelectricity and surface effect on the resonant frequency considering the effect of imperfections. This paper aims to highlight the influence of flexoelectricity and surface effects on the free vibration of an imperfect piezoelectric nanobeam in detail for various boundary conditions. In section 2 of this paper, the fundamentals of the flexoelectricity and the surface effect will be presented. In section 3, the governing equations will be expressed. Then, in section 4, the weakened effects will be considered in the structure, and finally, in section 5 the results will be shown and discussed.

2. Theory of flexoelectricity and the surface effect

As proposed by Shen and Hu [40] in order to take into account the surface effects, the beam would be decomposed into a bulk part and surface layers. In addition, in order to consider the flexoelectricity based on the extended linear theory for dielectrics, the terms of strain gradient, polarization, and polarization gradient are incorporated. Thus, for the bulk part, the general expression for the internal energy density U_b can be expressed as

$$\begin{aligned} U_b = {} & \frac{1}{2}a_{kl}P_kP_l + \frac{1}{2}b_{ijkl}P_{i,j}P_{k,l} + \frac{1}{2}c_{ijkl}\varepsilon_{ij}\varepsilon_{kl} + d_{ijk}\varepsilon_{ij}P_k + e_{ijkl}\varepsilon_{ij}P_{k,l} \\ & + f_{ijkl}u_{i,jk}P_l + r_{ijklm}\varepsilon_{ij}u_{k,lm} + \frac{1}{2}g_{ijklmn}u_{i,jk}u_{l,mn}\,, \end{aligned} \tag{1}$$

where P_i is the polarization vector, b_{ijkl} is the higher order coupling between the polarization gradient, ε_{ij} is the strain tensor which is defined as $\varepsilon_{ij} = \frac{1}{2}(u_{i,j} + u_{j,i})$; u_i is the displacement vector; a_{kl} is the reciprocal dielectric susceptibility; c_{ijkl} is the elastic constant; d_{ijk} is the piezoelectric coefficient, f_{ijkl} and e_{ijkl} are the direct and converse flexoelectric constant tensors, respectively.

For simplicity the coupling effects between strain and strain gradient are ignored and hence the elements r_{ijklm} and g_{ijklmn} are assumed to be zero [15]. Thereby, the constitutive equation can be expressed as

$$\begin{aligned} \sigma_{ij} &= \frac{\partial U_b}{\partial \varepsilon_{ij}} = c_{ijkl}\varepsilon_{kl} + d_{ijk}P_k + e_{ijlk}P_{k,l}\,, \\ \tau_{ijl} &= \frac{\partial U_b}{\partial \varepsilon_{ij,l}} = f_{ijlk}P_k\,, \\ E_i &= \frac{\partial U_b}{\partial P_i} = a_{ij}P_j + d_{jki}\varepsilon_{jk} + f_{jkli}\varepsilon_{jk,l}\,, \\ E_{ij} &= \frac{\partial U_b}{\partial P_{i,j}} = b_{ijkl}P_{k,l} + d_{klij}\varepsilon_{kl}\,, \end{aligned} \tag{2}$$

where σ_{ij}, τ_{ijl}, E_i, and E_{ij} are the stress, higher order stress, electric field and higher order electrical force, respectively. Gurtin and Murdoch [41] developed a continuum theory of the elastic material surfaces, and derived a linear theory considering the residual stress. Therefore, for the piezoelectric materials with surface effects, including the surface piezoelectricity, the residual surface stress and the surface elasticity, the surface internal energy density U_s depending on the surface polarization and the surface strain, can be expressed as [40, 42]

$$U_s = U_{s0} + \frac{1}{2}a^s_{\alpha\beta}P^s_\alpha P^s_\beta + \frac{1}{2}c^s_{\alpha\beta\gamma\kappa}\varepsilon^s_{\alpha\beta}\varepsilon^s_{\gamma\kappa} + d^s_{\alpha\beta\gamma}\varepsilon^s_{\alpha\beta}P^s_\gamma + \sigma^0_{\alpha\beta}\varepsilon^s_{\alpha\beta}\,, \tag{3}$$

in which $a^s_{\alpha\beta}$, $c^s_{\alpha\beta}$, and $d^s_{\alpha\beta\gamma}$ are the surface reciprocal dielectric susceptibility tensor, the surface elastic constant tensor and surface piezoelectric constant tensor, respectively. Also, P^s_α, $\varepsilon^s_{\alpha\beta}$, and $\sigma^0_{\alpha\beta}$ denote the surface polarization tensor, surface strain tensor, and residual surface stress tensor, respectively.

The surface constitutive equations can be determined as

$$\begin{aligned} \sigma^s_{\alpha\beta} &= \frac{\partial U_s}{\partial \varepsilon^s_{\alpha\beta}} = \sigma^0_{\alpha\beta} + c^s_{\alpha\beta\gamma\kappa}\varepsilon^s_{\gamma\kappa} + d^s_{\alpha\beta\gamma}P^s_\gamma, \\ E^s_\alpha &= \frac{\partial U_s}{\partial P^s_\alpha} = a^s_{\alpha\beta}P^s_\beta + d^s_{\beta\gamma\alpha}\varepsilon^s_{\beta\gamma}, \end{aligned} \tag{4}$$

where $\sigma^s_{\alpha\beta}$ and E^s_α are the surface stress tensor and surface electric field vector, respectively. The flexoelectricity can be written by the flexoelectric coefficient tensor ($\mu_{jkli} = f_{jkli} - e_{jkli}$) [43]. Moreover, according to [44] the direct and converse flexoelectric constant tensors are justified to satisfy $f_{ijkl} = -e_{ijkl}$.

3. Modeling and formulation

3.1. Governing equations within the Euler-Bernoulli beam framework

According to the Euler-Bernoulli beam theory, the displacement vector and axial elastic strain at any point of the piezoelectric nanobeam can be defined as

$$\mathrm{u}(x,t) = -\frac{\partial w(x,t)}{\partial x}\mathrm{e}_x + w(x,t)\mathrm{e}_z, \tag{5}$$

$$\varepsilon_{xx} = -z\frac{\partial^2 w(x,t)}{\partial x^2}, \tag{6}$$

where $\mathrm{x} = (x, y, z)$ are the spatial variables, w is the transverse displacement, and t denotes time. The constitutive equations for the bulk and surface of the one-dimensional beam from Eq. (2) and Eq. (4) can be stated as

$$\begin{aligned} \sigma_{xx} &= c_{11}\varepsilon_{xx} + d_{31}P_z - \frac{\mu_{31}}{2}P_{z,z}, \\ E_z &= a_{33}P_z + d_{31}\varepsilon_{xx} + \frac{\mu_{31}}{2}\varepsilon_{xx,z}; \end{aligned} \tag{7}$$

$$\begin{aligned} \sigma^s_{xx} &= \sigma^0_{11} + c^s_{11}\varepsilon^s_{xx} + d^s_{31}P^s_z, \\ E^s_x &= E^0_x. \end{aligned} \tag{8}$$

Based on the generalized Young-Laplace equations [45], the traction jumps are described as

$$T_x = \frac{\partial \sigma^s_{xx}}{\partial x}, \qquad T^{l,u}_z = \left(\frac{\sigma^s_{xx}}{r}\right)^{l,u} \tag{9}$$

in which the subscript u is the upper surface stress, the subscript l is the lower surface stress, and r is the symbol of radius curvature. By using Hamilton's principle, the governing equation can be derived as [46, 47]

$$\delta \int_0^T \{K - U + W\} \mathrm{d}t = 0, \tag{10}$$

where K and U are the kinetic energy and strain energy, and W is the work done by external loads. The governing equation for the beam can be derived from Eq. (10) as follows

$$\frac{\partial^2}{\partial x^2}(M + M_s + F) - bT_z^s + f(x,t) - \rho I_0 \frac{\partial^2 w}{\partial t^2} = 0, \tag{11}$$

where $I_0 = \int_A \mathrm{d}A$ and $M = \int_A \sigma_{xx} z \, \mathrm{d}A$, $F = \int_A \tau_{xxz} \, \mathrm{d}A$, and $M_s = \int_A \sigma_{xx}^s z \, \mathrm{d}A$ are the bending moments due to the Cauchy stress, higher order double stress, and surface stress, respectively. $T_z^s = (T_z^u - T_z^l)$ is a lateral load considering the surface effect. By substituting Eq. (5) into Eq. (10), the governing equation can be derived as

$$(EI)^* \frac{\mathrm{d}^4 w(x,t)}{\mathrm{d}x^4} - P \frac{\mathrm{d}^2 w(x,t)}{\mathrm{d}x^2} + f(x,t) + \rho I_0 \frac{\partial^2 w(x,t)}{\partial t^2} = 0. \tag{12}$$

Due to the influence of flexoelectricity and surface effects, the effective bending rigidity is defined as follows [17, 46]

$$(EI)^* = \frac{1}{12} bh^3 \left(\frac{e_{31}^2}{a_{33}} + c_{11} \right) \left(1 + \frac{3\mu_{31}^2}{h^2 \left(e_{31}^2 + a_{33} c_{11} \right)} + \frac{a_{33} c_{11}^s + e_{31} e_{31}^s}{e_{31}^2 + a_{33} c_{11}} \left(\frac{6}{h} + \frac{2}{b} \right) \right). \tag{13}$$

The bending rigidity of the classical piezoelectric beam is defined as

$$(EI)^{**} = \frac{1}{12} bh^3 \left(\frac{e_{31}^2}{a_{33}} + c_{11} \right). \tag{14}$$

The axial load, including $P_b = \int_A \sigma_{11} \, \mathrm{d}A$ and $P_s = 2(b+h)\sigma_{11}^0 + 2\left(1 + \frac{b}{h}\right) e_{31}^s V$, can be denoted as [17, 48]

$$P = P_b + P_s = 2(b+h)\sigma_{11}^0 + e_{31} bV + 2\left(\frac{b}{h} + 1 \right) e_{31}^s V. \tag{15}$$

3.2. Free vibration of a piezoelectric nanobeam

At first, we will obtain the vibration frequency of the piezoelectric nanobeam in order to validate the results with those presented by Liang et al. [17]; when the effect of imperfection is omitted from the equations, the results of this work and those in [17] should be the same. By considering the external force equal to zero, the governing equation for the free vibration of the piezoelectric nanobeam can be expressedby virtue of Eq. (12) as

$$(EI)^* \frac{\mathrm{d}^4 w(x,t)}{\mathrm{d}x^4} - P\frac{\mathrm{d}^2 w(x,t)}{\mathrm{d}x^2} + \rho I_0 \frac{\partial^2 w(x,t)}{\partial t^2} = 0. \tag{16}$$

In order to determine the free vibration behavior, the displacement is assumed as the following Fourier series

$$w(x) = \sum_{n=1}^{\infty} W_n \sin\frac{n\pi x}{l} e^{i\omega_n t}, \tag{17}$$

where ω_n is the vibration frequency, and W_n is the Fourier coefficients. By substituting Eq. (17) into Eq. (16), the governing equation for free vibration problem will be expressed as

$$\left[(EI)^* \left(\frac{n\pi}{l}\right)^4 + P\left(\frac{n\pi}{l}\right)^2 - \rho I_0 \omega_n^2\right] W_n = 0. \tag{18}$$

By solving Eq. (18), the expression of ω_n^2 can be computed

$$\omega_n^2 = \frac{(EI)^* \left(\frac{n\pi}{l}\right)^4 + P\left(\frac{n\pi}{l}\right)^2}{\rho I_0}. \tag{19}$$

The positive root of ω_n is the frequency of the simply supported nanobeam for various values of positive integer n. To obtain the resonance frequency of the piezoelectric nanobeam, a harmonic vibration has been used to rewrite the displacement as

$$w(x,t) = W(x)e^{i\omega t}. \tag{20}$$

By substituting Eq. (20) into Eq. (16), and using the dimensionless variables and constants as

$$\bar{W} = \frac{W}{l}, \quad \zeta = \frac{x}{l}, \quad \lambda^2 = \frac{\rho\omega^2 I_0 l^4}{(EI)^*}$$

the governing equation can be cast into the form

$$\bar{W}^{(4)}(\zeta) - q\bar{W}''(\zeta) - \lambda^2 \bar{W}(\zeta) = 0, \tag{21}$$

where $q = \dfrac{Pl^2}{(EI)^*}$, and λ^2 is the frequency parameter. The general solution for the differential Eq. (21) is obtained as

$$\bar{W}_1(\zeta) = c_1 \sinh[\alpha_1\zeta] + c_2 \cosh[\alpha_1\zeta] + c_3 \cos[\alpha_2\zeta] + c_4 \sin[\alpha_2\zeta], \tag{22}$$

where α_1 and α_2 are the roots of the characteristic equation

$$\alpha_{1,2} = \sqrt{\frac{\pm q + \sqrt{q^2 + 4\lambda^2}}{2}}. \tag{23}$$

The following equation that is directly extracted from literature [17] is the same Eq. (23)

$$\beta_{1,2} = \left(\frac{\pm N + \sqrt{N^2 + 4\rho\omega^2 I_0 (EI)_{\text{eff}}}}{2(EI)_{\text{eff}}}\right)^{1/2}, \tag{24}$$

where $N = P$, $(EI)^* = (EI)_{\text{eff}}$. As mentioned above, the roots of characteristic equation are compared with the result being given in [17] and completely coincide.

4. The weakened piezoelectric nanobeam model

The vibration of an imperfect piezoelectric nanobeam with length l, width b, thickness h, and different boundary conditions, considering the flexoelectricity and surface effect is under study in this section. A Cartesian coordinate system (x, y, z) is adopted to describe the beam position. The polar direction of the piezoelectric body is along the z-axis. The location of the defect, described as an edge crack, is specified at a distance l_c with related dimensionless variable $d = l_c/l$.

As shown in Fig. 1, the defected nanobeam is modeled as a rotational and longitudinal spring that connects two separated parts of the beam at the defect

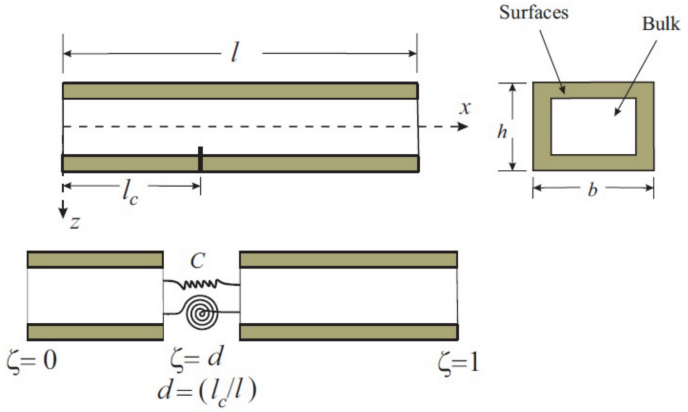

Fig. 1. Configuration of the cracked piezoelectric beam with surface effect

position. As a result, an additional strain energy will be caused by the spring [49]. So, the strain energy of a nanobeam weakened can be stated as

$$\Phi = \frac{1}{2}\int_0^l \left(N\frac{\partial v}{\partial x} + M\frac{\partial^2 u}{\partial x^2}\right) \mathrm{d}x + \Delta\Phi_c, \tag{25}$$

where $N = \int_A \sigma_{xx}\,\mathrm{d}A$ and $M = -\int_A y\,\sigma_{xx}\,\mathrm{d}A$ are the axial force and bending moment, and $\Delta\Phi_c$ is strain energy increasing due to the presence of the defect, can be written as

$$\Delta\Phi_c = \frac{1}{2}N\Delta u + \frac{1}{2}M\Delta\theta, \tag{26}$$

where $\Delta\theta$ and Δu are the angular displacement and horizontal displacement caused by rotational and longitudinal spring, respectively and may be expressed as

$$\begin{aligned} \Delta\theta &= c_{MM}\frac{\partial^2 u}{\partial x^2} + c_{MN}\frac{\partial v}{\partial x}, \\ \Delta u &= c_{NN}\frac{\partial v}{\partial x} + c_{NM}\frac{\partial^2 u}{\partial x^2}, \end{aligned} \tag{27}$$

where c_{MM}, c_{MN}, c_{NN}, c_{NM} are the flexibility constants. These constants which introduce the crack severity are considered as a hypothetical input in studies regarding to static and dynamic behaviors of nanobeams in the presence of a crack [50]. To study the free transverse vibration, the longitudinal displacement is neglected in this study. Besides, due to the low values of c_{MN} and c_{NM}, only c_{MM}, which corresponds with the bending moment, is considered in the equations. By using dimensionless variables, $\Delta\theta$ in the defect position is stated as

$$\Delta\theta = \frac{c_{MM}}{l}\left.\frac{\partial^2 \bar{U}}{\partial x^2}\right|_{\zeta=d} = C\left.\frac{\partial^2 \bar{U}}{\partial x^2}\right|_{\zeta=d}. \tag{28}$$

To analyze the free vibration of the imperfect nanobeam, governing equation of each segments of the nanobeam can be defined as follows by view of Eq. (21)

$$\begin{aligned} &\bar{W}^{(4)}(\zeta) - q\bar{W}''(\zeta) - \lambda^2\bar{W}(\zeta) = 0, \qquad 0 \leqslant \zeta \leqslant d, \\ &\bar{W}^{(4)}(\zeta) - q\bar{W}''(\zeta) - \lambda^2\bar{W}(\zeta) = 0, \qquad d \leqslant \zeta \leqslant 1. \end{aligned} \tag{29}$$

Therefore, general solution for each part can be expressed as

$$\begin{aligned} \bar{W}_1(\zeta) &= c_1\sinh\left[\beta_1\zeta\right] + c_2\cosh\left[\beta_1\zeta\right] + c_3\cos\left[\beta_2\zeta\right] + c_4\sin\left[\beta_2\zeta\right], \\ &\qquad\qquad 0 \leqslant \zeta \leqslant d, \\ \bar{W}_2(\zeta) &= d_1\sinh\left[\beta_1\zeta\right] + d_2\cosh\left[\beta_1\zeta\right] + d_3\cos\left[\beta_2\zeta\right] + d_4\sin\left[\beta_2\zeta\right], \\ &\qquad\qquad d \leqslant \zeta \leqslant 1. \end{aligned} \tag{30}$$

The mentioned equations, including eight unknown constants, are solved using the boundary conditions and compatibility conditions at the defect position

$$\begin{aligned} \bar{W}_2(d) &= \bar{W}_1(d), \quad \bar{W}_2'(d) - \bar{W}_1'(d) = K\bar{W}_1''(d), \\ \bar{W}_2''(d) &= \bar{W}_1''(d), \quad \bar{W}_2'''(d) = \bar{W}_1'''(d). \end{aligned} \tag{31}$$

By applying the different boundary conditions and above conditions into the Eq. (30), the resonance frequencies are obtained.

5. Numerical results and discussion

In this section, numerical results of the vibration behavior of a weakened piezoelectric nanobeam considering the surface effects and flexoelectricity will be presented. The numerical calculations are conducted to illustrate the influence of six different boundary conditions, different positions of the defect, various crack severities, and thickness on the resonance frequency. PZT-5H and $BaTiO_3$ are used as samples of the piezoelectric materials.

Remarks

- Throughout this paper, the length to thickness ratio of the nanobeam is fixed at $l/h = 10$.
- Except for Fig. 10 there is no applied voltage ($V = 0$ V).
- Unlike Fig. 7 in which C changes, for other figures: C = 1.5.
- The residual surface stress could also change from a negative value to a positive value based on the crystal plane direction [44].
- In the presented results, symbols S-S, F-F, C-C, C-F, C-S and S-F are served to represent the simply supported, free, clamped, clamped-free, clamped-simply supported and simply supported-free beams.

In Table 1, the bulk material properties and the flexoelectric coefficient relevant to this study are determined by atomistic simulations or experiments, and the piezoelectric and surface elastic constants are obtained from [17, 51, 52].

Table 1.

The material properties

Properties	$\rho\ \left(\frac{\text{kg}}{\text{m}^3}\right)$	$c_{11}\ \left(\frac{\text{N}}{\text{m}^2}\right)$	$e_{31}\ \left(\frac{\text{C}}{\text{m}^2}\right)$	$a_{33}\ \left(\frac{\text{C}}{\text{Vm}}\right)$	$c_{11}^s\ \left(\frac{\text{N}}{\text{m}}\right)$	$e_{31}^s\ \left(\frac{\text{C}}{\text{m}}\right)$	$\mu_{31}\ \left(\frac{\text{C}}{\text{m}}\right)$
$BaTiO_3$	6020	131×10^9	1.87×10^8	0.79×10^8	9.72	−0.056	5×10^{-7}
PZT-5H	7500	126×10^9	−6.5	1.3×10^{-8}	7.56	-3×10^{-8}	5×10^{-7}

For the sake of validations, the normalized resonance frequency of a perfect piezoelectric nanobeam is compared with the results given by Liang et al. [17]. It is seen, Fig. 2, that the present results have an excellent agreements with those in [17]. It is observed when the beam thickness decreases, the influence of surface effect and flexoelectricity, size-dependent properties, on resonance frequency is more prominent within the two different values of residual surface stress.

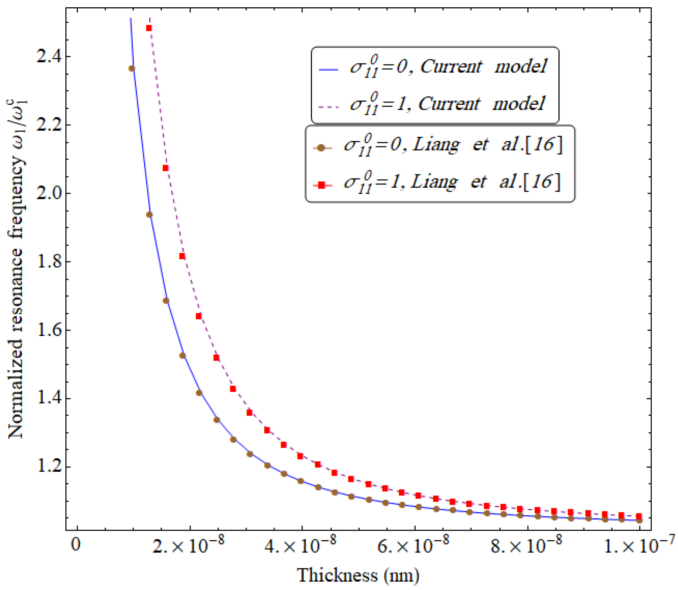

Fig. 2. Variation of the normalized resonance frequency versus thickness for a PZT-5H nanobeam, and S-S beam

The results in Fig. 3 have shown in displays the critical influence of boundary conditions on the resonance frequency for PZT-5H nanobeam. It is shown that the surface effect at the resonance frequency depends on boundary conditions and defect position, and is more announced for F-F and C-C beams. It is determined that the resonance frequency for C-F beam is lower than those obtained without the surface effects as opposed to C-C and S-S beams. Interestingly, it is observed that C-C, F-F, and S-S beams present a softer-like elastic behavior, while C-F condition indicates a stiffer-like elastic behavior.

According to the results depicted in Fig. 4, the maximum values of the normalized resonance frequency for both C-S and S-F nanobeam are similar. In this example, both surface and flexoelectricity effects are taken into account. For S-F beam, when the defect is located at $\zeta = 0.4$, resonance frequency hits its lowest values, while for C-S beam the lowest resonance frequency occurs at $\zeta = 0.7$.

In Fig. 5, the resonance frequency for the $BaTiO_3$ nanobeam considering the surface effects is shown. It can be seen that the effect of the residual surface stress is significant. Also, using different values of residual surface stress in the mentioned numerous investigations in the literature [52] confirm this explanation. It is noteworthy to mention that the resonance frequency decreases by moving to $\zeta = 0.5$ and then increases in a symmetric manner.

Fig. 6 represents the effect of flexoelectricity. The variation of the resonance frequency with the crack position is plotted while this effect is taken into account. It is apparent from this figure that the flexoelectricity decreases the resonance

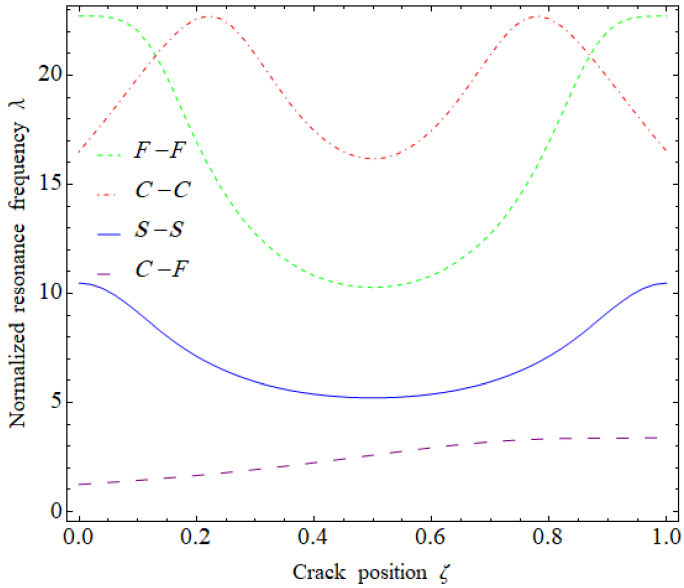

Fig. 3. Variation of the normalized resonance frequency with the crack position for a PZT-5H beam with various boundary conditions (F-F, C-C, S-S, and C-F) and $\sigma_{11}^{0} = 1\ \mathrm{N\,m^{-2}}$

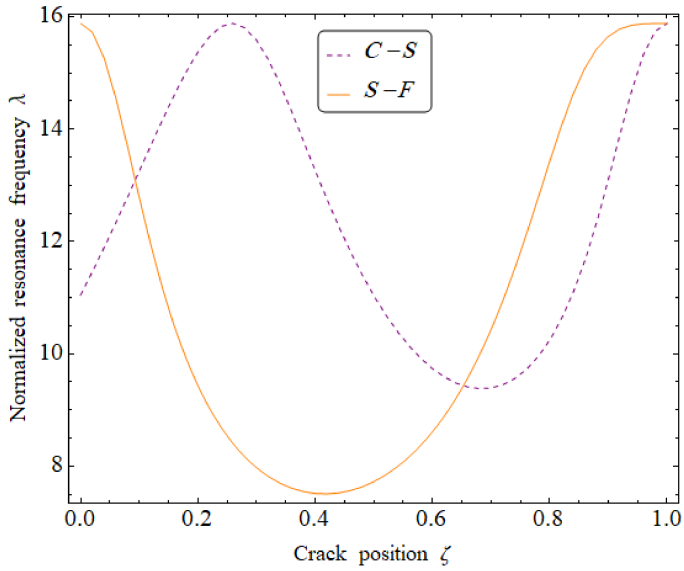

Fig. 4. Variation of the normalized resonance frequency with the crack position for a PZT-5H beam with different boundary conditions (C-S and S-F) and $\sigma_{11}^{0} = 1\ \mathrm{N\,m^{-2}}$

frequency of S-S beam, and this influence is suppressed while there is a defect. For C-F beam, unlike the previous condition, the flexoelectricity enhances the resonance frequency. Moreover, the flexoelectric effect is more considerable in

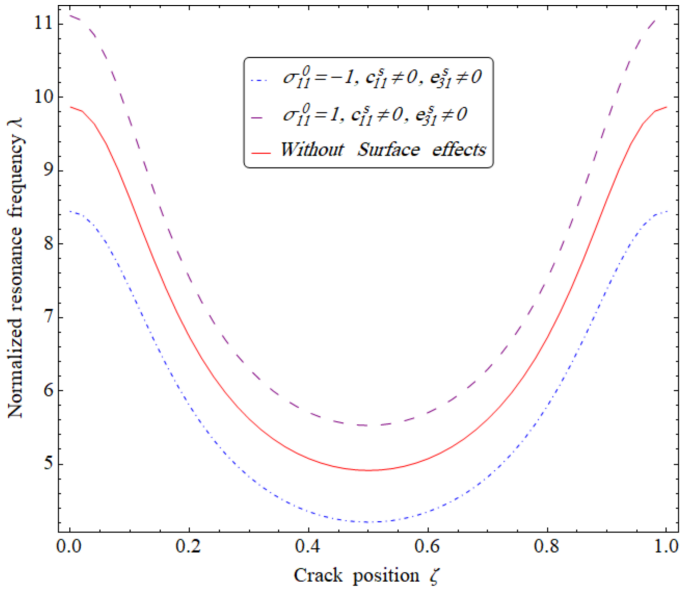

Fig. 5. Variation of the normalized resonance frequency with the crack position for a $BaTiO_3$ and S-S nanobeam considering surface effects

S-S beam than C-F beam. So, the flexoelectric effect on the vibration behavior of the piezoelectric nanobeam is sensitive to the beam boundary conditions. For the

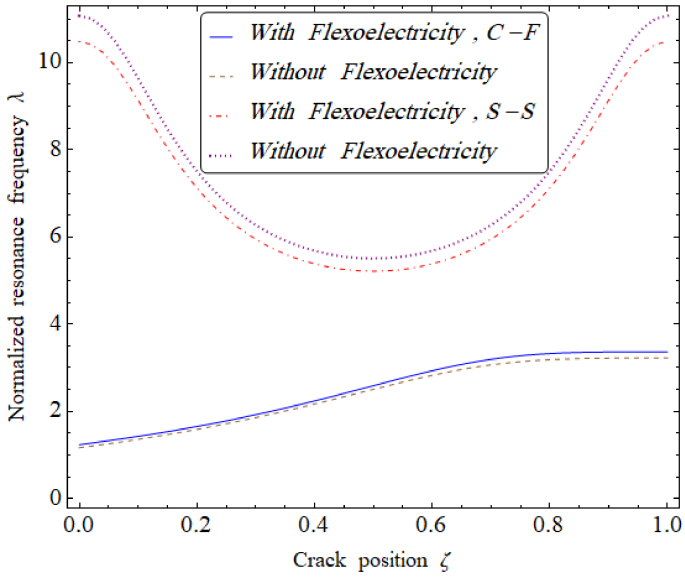

Fig. 6. Variation of the normalized resonance frequency with the crack position for a PZT-5H nanobeam, and for S-S, and C-F beams and $\sigma_{11}^0 = 1\ \mathrm{N\,m^{-2}}$

S-S beam, when the crack is located at the midpoint of the beam, the resonance frequency hits its minimum value.

Fig. 7 represents the effect of the crack position on resonance frequency considering the flexoelectricity and surface effects. The resonance frequency is equal for all crack severities when a crack located at $\zeta = 0$ and $\zeta = 1$ that indicates the perfect beam. The resonance frequency is minima while the defect is located at the middle of the beam ($\zeta = 0.5$). According to the results, as the crack severity increases, the difference between the two consecutive curves decreases. The inverse relationship between the resonance frequency and the crack severity was also discussed in [19, 49].

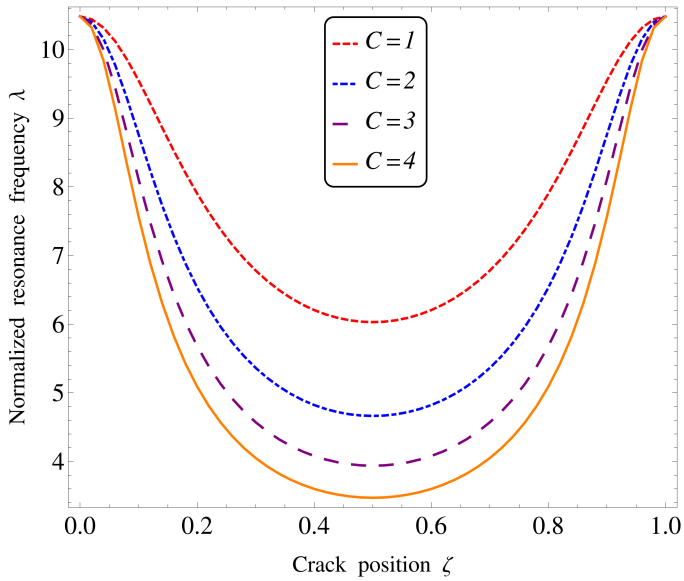

Fig. 7. Variation of the normalized resonance frequency with the crack position for a PZT-5H nanobeam, and for the S-S beam and $\sigma^0_{11} = 1\ \mathrm{N\,m^{-2}}$

The effect of thecrack severity on the resonance frequency considering the surface effect and flexoelectricity is plotted in Fig. 8. The defect is located at $\zeta = 0.25$. Results demonstrate that the frequency of the nanobeam decreases drastically as the crack severity increases [53]. Furthermore, the resonance frequency value caused by $BaTiO_3$ nanobeam is more than PZT-5H that is justified by the material properties of Table 1.

Fig. 9 represents the normalized resonance frequency versus the crack position taking into account the flexoelectricty effect. As presented in the figure, flexoelectricity decreases the normalized resonance frequency of S-S beam, and this influence enhances while the geometry effect (b/h) increases. It is observed that the resonance frequency almost remains the same for $b/h = 0.25$. The size dependency of flexoelectricity is illustrated in this figure as well. As long as the

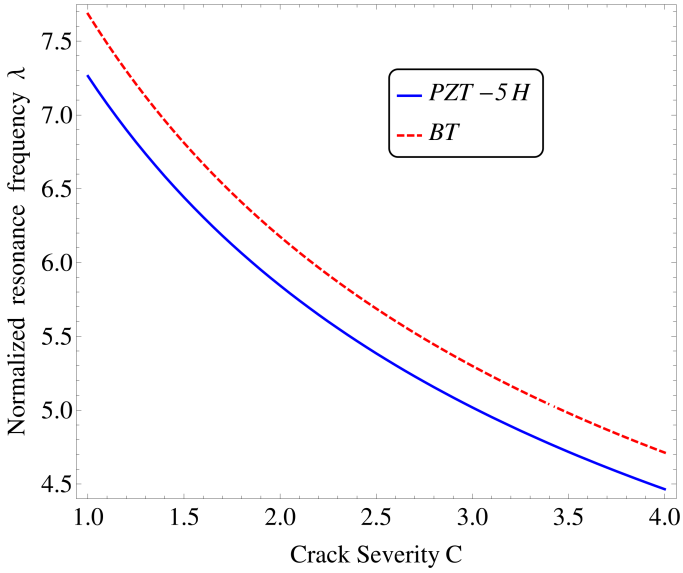

Fig. 8. Variation of the normalized resonance frequency *versus* crack severity for the S-S beam with two different piezoelectric materials, while $\sigma_{11}^{0} = 1\ \mathrm{N\,m^{-2}}$, $V = 0$ V, and $\zeta = 0.25$

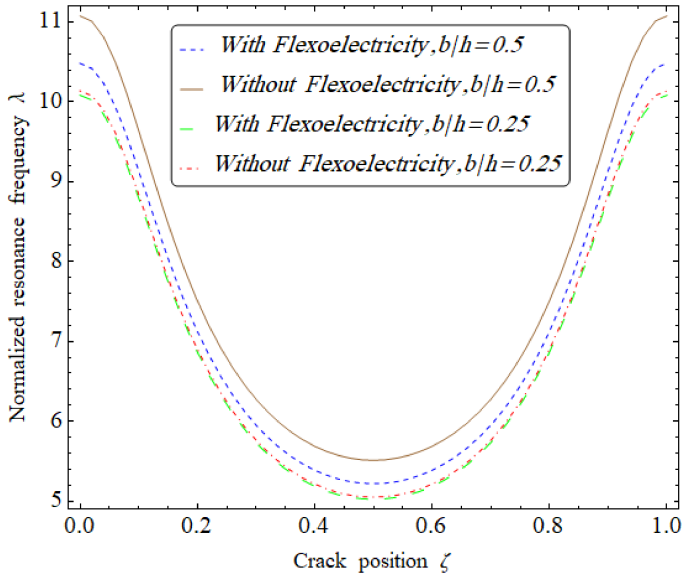

Fig. 9. Variation of the normalized resonance frequency with the crack position for a PZT-5H nanobeam and for S-S beam with flexoelectric effect, while $\sigma_{11}^{0} = 1$

defect moves along the nanobeam, the resonance frequency decreases, and the resonance frequency takes the lowest value when the defect is located in the middle of the nanobeam.

Fig. 10 analyzes the behavior of S-S and C-F beams subjected to the different values of voltage. In this figure, the normalized resonance frequency versus the crack position is shown, while there is no residual surface stress. The most surprising aspect of the results is that the influence of the voltage on the resultant resonance frequency depends on the physical boundary conditions. A comprasion of results reveals that for S-S condition the resonance frequency is lower for the positive in contrast to the C-F condition. In S-S condition, by increasing the distance of imperfection from two ends of the nanobeam, the resonance frequency decreases and it reaches its lowest value at the midpoint. On the contrary, for C-F nanobeam, the lowest value of the resonance frequency occurs in the left corner of the beam.

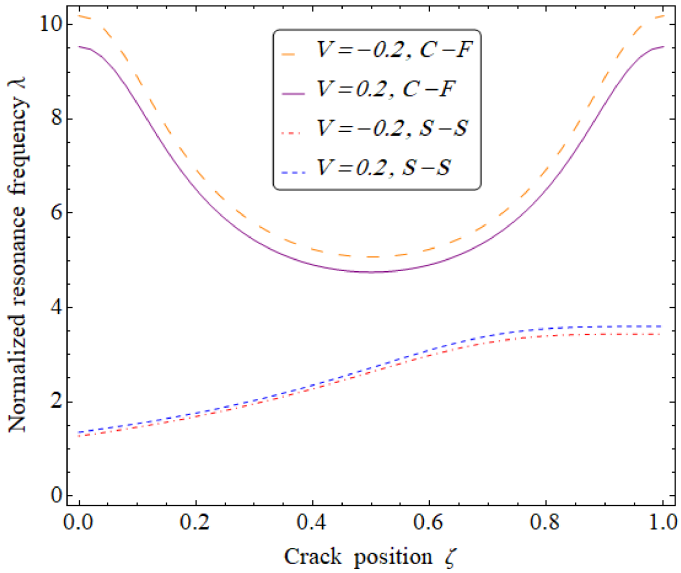

Fig. 10. Variation of the normalized resonance frequency with the crack position for a PZT-5H nanobeam, and for S-S and C-F beams, and $\sigma_{11}^{0} = 0$

6. Conclusions

In the presented paper, the Euler-Bernoulli beam model incorporating the surface effects and flexoelectricity is used to investigate the size-dependent properties of the vibration behavior of an imperfect piezoelectric nanobeam. The modeling of a cracked nanobeam was performed using a rotational and a longitudinal spring. The resonance frequencies for the free vibration of the weakened piezoelectric nanobeam for various different boundary conditions were studied. The results indicate that the surface effects considering the residual surface stress, surface elasticity, surface piezoelectricity, flexoelectricity, defect position and crack severity highly

affect the mechanical behaviors of the weakened piezoelectric nanobeam. It can also be concluded that the surface effect and the flexoelectricity are size-dependent and are far more dominant when thickness of the nanobeam tends to small values. It is found that C-F condition provides softer-like elastic behavior compared to other boundary condition types. Additionally, the results suggest that as long as crack severity increases, the normalized resonance frequency decreases.

Manuscript received by Editorial Board, April 05,2019;
final version, November 04, 2019.

References

[1] S.M. Tanner, J.M. Gray, C.T. Rogers, K.A. Bertnees, and N.A. Sanford. High-Q GaN nanowire resonators and oscillators. *Applied Physics Letters*, 91(20):203117, 2007. doi: 10.1063/1.2815747.

[2] W.S. Su, Y.F. Chen, C.L. Hsiao, and L.W. Tu. Generation of electricity in GaN nanorods induced by piezoelectric effect. *Applied Physics Letters*, 90(6):063110, 2007. doi: 10.1063/1.2472539.

[3] B. Kumar and S.-W. Kim. Energy harvesting based on semiconducting piezoelectric ZnO nanostructures. *Nano Energy*, 1(3):342–355, 2012. doi: 10.1016/j.nanoen.2012.02.001.

[4] Z.L. Wang and J. Song. Piezoelectric nanogenerators based on zinc oxide nanowire arrays. *Science*, 312(5771):242–246, 2006. doi: 10.1126/science.1124005.

[5] X. Wang, J. Zhou, J. Song, J. Liu, N. Xu, and Z.L.Wang. Piezoelectric field effect transistor and nanoforce sensor based on a single ZnO nanowire. *Nano Letters*, 6(12):2768–2772, 2006. doi: 10.1021/nl061802g.

[6] S.C. Lao, Q. Kuang, Z.L. Wang, M.C. Park, and Y. Deng. Polymer functionalized piezoelectric-FET as humidity/chemical nanosensors. *Applied Physics Letters*, 90(26): 262107, 2007. doi: 10.1063/1.2748097.

[7] A. Chaipanich. Effect of PZT particle size on dielectric and piezoelectric properties of PZT–cement composites. *Current Applied Physics*, 7(5):574–577, 2007. doi: 10.1016/j.cap.2006.11.036.

[8] H. Farokhi, A.K. Misra, and M.P. Païdoussis. A new electrostatic load model for initially curved carbon nanotube resonators: pull-in characteristics and nonlinear resonant behaviour. *Nonlinear Dynamics*, 88(2):1187–1211, 2017. doi: 10.1007/s11071-016-3304-1.

[9] Z. Zhang, Z. Yan, and L. Jiang. Flexoelectric effect on the electroelastic responses and vibrational behaviors of a piezoelectric nanoplate. *Journal of Applied Physics*, 116(1): 014307, 2014. doi: 10.1063/1.4886315.

[10] X. Liang, S. Hu, and S. Shen. Effects of surface and flexoelectricity on a piezoelectric nanobeam. *Smart Materials and Structures*, 23(3):035020, 2014. doi: 10.1088/0964-1726/23/3/035020.

[11] Z. Yan. Size-dependent bending and vibration behaviors of piezoelectric circular nanoplates. *Smart Materials and Structures*, 25(3): 035017, 2016. doi: 10.1088/0964-1726/25/3/035017.

[12] T.D. Nguyen, S. Mao, Y. Yeh , P.K. Purohit, and M.C. McAlpine. Nanoscale flexoelectricity. *Advanced Materials*, 25(7):946–974, 2013. doi: 10.1002/adma.201203852.

[13] L. Qi, S. Zhou, and A. Li. Size-dependent bending of an electro-elastic bilayer nanobeam due to flexoelectricity and strain gradient elastic effect. *Composite Structures*, 135:167–175, 2016. doi: 10.1016/j.compstruct.2015.09.020.

[14] R. Zhang, X. Liang, and S. Shen. A Timoshenko dielectric beam model with flexoelectric effect. *Meccanica*, 51(5):1181–1188, 2016. doi: 10.1007/s11012-015-0290-1.

[15] Z. Yan and L.Y. Jiang. Flexoelectric effect on the electroelastic responses of bending piezoelectric nanobeams. *Journal of Applied Physics*. 113(19):194102, 2013. doi: 10.1063/1.4804949.

[16] Z. Zhang. *Size-dependent Electroelastic Properties of Piezoelectric Nanoplates*. Master Thesis, The University of Western Ontario, Canada, 2014.

[17] X. Liang, S.Hu, and S. Shen. Size-dependent buckling and vibration behaviors of piezoelectric nanostructures due to flexoelectricity. *Smart Materials and Structures*, 24(10):105012, 2015. doi: 10.1088/0964-1726/24/10/105012.

[18] Y. Tadi Beni. Size-dependent analysis of piezoelectric nanobeams including electromechanical coupling. *Mechanics Research Communications*, 75: 67–80, 2016. doi: 10.1016/j.mechrescom.2016.05.011.

[19] R. Sourki and S.A.H. Hoseini. Free vibration analysis of size-dependent cracked microbeam based on the modified couple stress theory. *Applied Physics A*, 122(4):413, 2016. doi: 10.1007/s00339-016-9961-6.

[20] R. Sourki and S.A. Hosseini. Coupling effects of nonlocal and modified couple stress theories incorporating surface energy on analytical transverse vibration of a weakened nanobeam. *The European Physical Journal Plus*, 132(4):184, 2017. doi: 10.1140/epjp/i2017-11458-0.

[21] S.J. Behrouz, O. Rahmani, and S.A. Hosseini. On nonlinear forced vibration of nano cantilever-based biosensor via couple stress theory. *Mechanical Systems and Signal Processing*, 128: 19–36, 2019. doi: 10.1016/j.ymssp.2019.03.020.

[22] B.A. Hamidi, S.A.H. Hosseini, R. Hassannejad, and F. Khosravi. An exact solution on gold microbeam with thermoelastic damping via generalized Green-Naghdi and modified couple stress theories. *Journal of Thermal Stresses*, 2019. doi: 10.1080/01495739.2019.1666694.

[23] S.A Hosseini and O. Rahmani. Modeling the size effect on the mechanical behavior of functionally graded curved micro/nanobeam. *Thermal Science and Engineering*, 1(2):1–20, 2018. doi: 10.24294/tse.v1i2.400.

[24] O. Rahmani, M. Shokrnia, H. Golmohammadi, and S.A.H. Hosseini. Dynamic response of a single-walled carbon nanotube under a moving harmonic load by considering modified nonlocal elasticity theory. *The European Physical Journal Plus*, 133(2):42, 2018. doi: 10.1140/epjp/i2018-11868-4.

[25] M. Ghadiri, S. Hosseini, M. Karami, and M. Namvar. In-plane and out of plane free vibration of U-shaped AFM probes based on the nonlocal elasticity. *Journal of Solid Mechanics Vol*, 10(2):285–299, 2018.

[26] S. Hosseini and O. Rahmani. Bending and vibration analysis of curved FG nanobeams via nonlocal Timoshenko model. *Smart Construction Research*, 2(2):1–17, 2018.

[27] M. Namvar, E. Rezaei, S.A. Hosseini, and M. Ghadiri. Experimental and analytical investigations of vibrational behavior of U-shaped atomic force microscope probe considering thermal loading and the modified couple stress theory. *The European Physical Journal Plus*, 132(6): 247, 2017. doi: 10.1140/epjp/i2017-11518-5.

[28] V. Refaeinejad, O. Rahmani, and S.A.H. Hosseini. Evaluation of nonlocal higher order shear deformation models for the vibrational analysis of functionally graded nanostructures. *Mechanics of Advanced Materials and Structures*, 24(13):1116–1123, 2017. doi: 10.1080/15376494.2016.1227496.

[29] M. Zarepour, S.A.H. Hosseini, and A.H. Akbarzadeh. Geometrically nonlinear analysis of Timoshenko piezoelectric nanobeams with flexoelectricity effect based on Eringen's differential model. *Applied Mathematical Modelling*, 69:563–582, 2019. doi: 10.1016/j.apm.2019.01.001.

[30] C. Zhang, J. Zhu, W. Chen, and Ch. Zhang. Two-dimensional theory of piezoelectric shells considering surface effect. *European Journal of Mechanics – A/Solids*, 43:109–117, 2014. doi: 10.1016/j.euromechsol.2013.09.007.

[31] Z. Zhang and L. Jiang. Size effects on electromechanical coupling fields of a bending piezoelectric nanoplate due to surface effects and flexoelectricity. *Journal of Applied Physics*, 116(13):134308, 2014. doi: 10.1063/1.4897367.

[32] Z. Yan and L. Jiang. Surface effects on the electroelastic responses of a thin piezoelectric plate with nanoscale thickness. *Journal of Physics D: Applied Physics*, 45(25):255401, 2012. doi: 10.1088/0022-3727/45/25/255401.

[33] G.Y. Huang and S.W. Yu. Effect of surface piezoelectricity on the electromechanical behaviour of a piezoelectric ring. *Physica Status Solidi b*, 243(4):R22-R24, 2006. doi: 10.1002/pssb.200541521.

[34] Y.S. Li and E. Pan. Bending of a sinusoidal piezoelectric nanoplate with surface effect. *Composite Structures*, 136:45–55, 2016. doi: 10.1016/j.compstruct.2015.09.047.

[35] M.S. Chiu. and T. Chen. Effects of high-order surface stress on static bending behavior of nanowires. *Physica E: Low-dimensional Systems and Nanostructures*, 44(3):714–718, 2011. doi: 10.1016/j.physe.2011.11.016.

[36] A.H. Hosseini, O. Rahmani, M. Nikmehr, I.F. Golpayegani. Axial vibration of cracked nanorods embedded in elastic foundation based on a nonlocal elasticity model. *Sensor Letters*, 14(10):1019–1025, 2016. doi: 10.1166/sl.2016.3575.

[37] O. Rahmani, S.A.H. Hosseini, M.H.N. Moghaddam, and I.F. Golpayegani. Torsional vibration of cracked nanobeam based on nonlocal stress theory with various boundary conditions: An analytical study. *International Journal of Applied Mechanics*, 07(03):1550036, 2015. doi: 10.1142/S1758825115500362.

[38] J. Xiao, Y. Xu, and F. Zhang. A rigorous solution for the piezoelectric materials containing elliptic cavity or crack with surface effect. *ZAMM – Journal of Applied Mathematics and Mechanics / Zeitschrift für Angewandte Mathematik und Mechanik*, 96(5):633–641, 2016. doi: 10.1002/zamm.201400232.

[39] K.F. Wang, and B.L. Wang. Nonlinear fracture mechanics analysis of nano-scale piezoelectric double cantilever beam specimens with surface effect. *European Journal of Mechanics – A/Solids*, 56:12–18, 2016. doi: 10.1016/j.euromechsol.2015.10.002.

[40] H.S. Nan and B.L. Wang. Effect of crack face residual surface stress on nanoscale fracture of piezoelectric materials. *Engineering Fracture Mechanics*, 110:68–80, 2013. doi: 10.1016/j.engfracmech.2013.08.002.

[41] S. Shen and S. Hu. A theory of flexoelectricity with surface effect for elastic dielectrics. *Journal of the Mechanics and Physics of Solids*, 58(5):665–677, 2010. doi: 10.1016/j.jmps.2010.03.001

[42] M. E. Gurtin and A.I. Murdoch. A continuum theory of elastic material surfaces. *Archive for Rational Mechanics and Analysis*, 57(4):291–323, 1975. doi: 10.1007/BF00261375.

[43] J. Zhang, C. Wang, and S. Adhikari. Surface effect on the buckling of piezoelectric nanofilms. *Journal of Physics D: Applied Physics*, 45(28):285301, 2012. doi: 10.1088/0022-3727/45/28/285301.

[44] A. Abdollahi, C. Peco, D. Millán, M. Arroyo, and I. Arias. Computational evaluation of the flexoelectric effect in dielectric solids. *Journal of Applied Physics*, 116(9):093502, 2014. doi: 10.1063/1.4893974.

[45] Z. Zhang and L. Jiang. Size effects on electromechanical coupling fields of a bending piezoelectric nanoplate due to surface effects and flexoelectricity. *Journal of Applied Physics*, 116(13):134308, 2014. doi: 10.1063/1.4897367.

[46] T. Chen, M.S. Chiu, and C.N. Weng. Derivation of the generalized Young-Laplace equation of curved interfaces in nanoscaled solids. *Journal of Applied Physics*, 100(7):074308, 2006. doi: 10.1063/1.2356094.

[47] Z. Yan and L. Jiang. Influence of surface effects and flexoelectricity on vibration of piezoelectric nanobeams. *13th International Conference on Fracture*, Beijing, China, 16–21 June, 2013.

[48] X. Liang, S. Hu, and S. Shen. A new Bernoulli–Euler beam model based on a simplified strain gradient elasticity theory and its applications. *Composite Structures*, vol. 111:317–323, 2014. doi: 10.1016/j.compstruct.2014.01.019.

[49] Z. Yan and L.Y. Jiang. The vibrational and buckling behaviors of piezoelectric nanobeams with surface effects. *Nanotechnology*, 22(24):245703, 2011. doi: 10.1088/0957-4484/22/24/245703.

[50] J. Loya, J. López-Puente, R. Zaera, and J. Fernández-Sáez. Free transverse vibrations of cracked nanobeams using a nonlocal elasticity model. *Journal of Applied Physics*, 10(4):044309, 2009. doi: 10.1063/1.3068370.

[51] M. Akbarzadeh Khorshidi and M. Shariati. Investigation of flexibility constants for a multi-spring model: a solution for buckling of cracked micro/nanobeams. *Journal of Theoretical and Applied Mechanics*, vol. 57(1):49–58, 2019.

[52] L.L. Zhang, J.X. Liu, X.Q. Fang, and G.Q. Nie. Effects of surface piezoelectricity and nonlocal scale on wave propagation in piezoelectric nanoplates. *European Journal of Mechanics – A/Solids*, 46:22–29, 2014. doi: 10.1016/j.euromechsol.2014.01.005.

[53] Y.M. Yue, K.Y. Xu, and T. Chen. A micro scale Timoshenko beam model for piezoelectricity with flexoelectricity and surface effects. *Composite Structures*, 136:278–286, 2016. doi: 10.1016/j.compstruct.2015.09.046.

[54] J.A. Loya, J. Aranda-Ruiz, and J. Fernández-Sáez. Torsion of cracked nanorods using a nonlocal elasticity model. *Journal of Physics D: Applied Physics*, 47(11):115304, 2014. doi: 10.1088/0022-3727/47/11/115304.